



Influence of the deposition technique on the structural and optical properties of amorphous As–S films

J.M. González-Leal^{a,*}, M. Stuchlik^b, M. Vlcek^c, R. Jiménez-Garay^a, E. Márquez^b

^a*Departamento de Física de la Materia Condensada, Facultad de Ciencias, Universidad de Cádiz, 11510 Puerto Real (Cádiz), Spain*

^b*Department of Chemistry, University of Cambridge, Lensfield Road, CB21EW Cambridge, UK*

^c*Department of General and Inorganic Chemistry, University of Pardubice, 53210 Pardubice, Czech Republic*

Available online 15 January 2005

Abstract

Amorphous chalcogenide films of stoichiometric composition $\text{As}_{40}\text{S}_{60}$ have been prepared by three different deposition techniques, namely, vacuum thermal evaporation, plasma-enhanced chemical vapour deposition (PECVD) and spin coating. Indications of film-thickness inhomogeneities were found in all samples. Thermally evaporated and chemically deposited samples showed wedge-shaped surface profiles, while significant surface roughness was evidenced in the spin-coated ones. Refractive-index values of the film samples were obtained, with accuracy better than 1%, by using the envelope method most suitable for each particular film surface profile. Structural information of the samples has been gained from X-ray diffraction experiments, and also inferred from the analysis of the dispersion of the refractive index, on the basis of a single-oscillator model. Analysis of the optical absorption spectra allowed both calculating the optical band gaps and estimating the localised-state tail width of these semiconducting films. In addition, information about the degree of structural randomness of these thin-film amorphous alloys was also obtained from this analysis, which is in good agreement with the conclusions derived from the X-ray diffraction results.

© 2004 Elsevier B.V. All rights reserved.

Keywords: As–S films; Thermal evaporation; Spin coating; PECVD

1. Introduction

It is well known that the conditions for material preparation play a crucial role in its properties, mainly in the case of thin-film samples [1–3]. Therefore, to

achieve a good reproduction in the material properties, all the parameters involved in the deposition technique must be controlled. Thus, for instance, the deposition rate has a great influence on the compactness of thermally evaporated films, the chemical composition of the films prepared by plasma-enhanced chemical vapour deposition (PECVD) strongly depends on the volume ratio of precursor gases, and the spin speed has a significant effect in the compositional homogeneity of spin-coated films.

* Corresponding author. Tel.: +34 956 016748;

fax: +34 956 016288.

E-mail address: juanmaria.gonzalez@uca.es
(J.M. González-Leal).

Chalcogenide glasses have been attracting the interest of researchers and engineers during the last decades, to both answer questions about the physics of the amorphous semiconductors [4], and use their properties and the photo-induced metastabilities that they present, in a number of technological applications dealing with data recording media, sensors, optical communications and integrated optics [5,6], among a number of others. The structural versatility of these materials, which is ultimately behind their unique features, concurrently makes them strongly dependent on the preparation technique. The aim of the present paper is to report on the influence of the film deposition technique on both the structural and optical properties of thin films of amorphous As–S alloys, prepared by vacuum thermal evaporation, PECVD, and spin coating.

2. Experimental

Stoichiometric As_2S_3 chalcogenide bulk samples were prepared by direct synthesis from high-purity elements (5N), heated together in an evacuated quartz ampoule, at a temperature of approximately 900 °C, for about 24 h. After the synthesis, the melt was air quenched. Thin-film samples were deposited onto clean, weakly absorbing glass substrates (microscope slides), from the powdered bulk starting material, by both vacuum thermal evaporation, performed within a coating system (Tesla Corporation, model UP-858) at a pressure of about 10^{-3} Pa [7], and spin coating, from 0.8 M solutions of the bulk starting material in *n*-propylamine ($CH_3CH_2CH_2-NH_2$) [8].

On the other hand, amorphous As_2S_3 thin films were also deposited by PECVD, from high-purity H_2S and AsH_3 hydrides, in a plasma-discharge stainless steel reactor, by use of an rf discharge (13.56 MHz) between two parallel plate electrodes, 8 cm in diameter. The distance between the electrodes was 3 cm for all the depositions carried out. Electronic mass flow controllers were used in order to control gas flows. The total gas pressure was measured and automatically regulated through a butterfly valve by a Baratron pressure gauge. Clean glass substrates were fixed on both electrodes. Depositions were made without additional heating of the substrate, but due to unintentional heating by the plasma, the temperature

may rise up to approximately 50 °C. The precursor gases were introduced in the reaction chamber setting the gas flow at 10 sccm. Amorphous films of stoichiometric composition were obtained at 0.20 mbar, $AsH_3/H_2S = 1/19$, and an rf power of 15 W.

X-ray diffraction measurements were carried out by means of a diffractometer (Phillips, model PW 1870), using Cu $K\alpha$ radiation ($\lambda = 1.54 \text{ \AA}$). No crystalline peaks were found in the X-ray diffraction patterns, proving the amorphous character of the samples. Electron microprobe analysis showed the actual chemical composition to be $As_{36.0 \pm 0.8}S_{63.6 \pm 0.7}$ for the thermally evaporated ones, $As_{35.7 \pm 1.8}S_{64.3 \pm 1.7}$ for those prepared by spin coating, and $As_{39.8 \pm 1.6}S_{60.3 \pm 1.8}$ for the PECVD deposited. Despite these compositional differences, the stoichiometric $As_{40}S_{60}$ composition, in at.%, will be used hereafter as representative, for all the samples, to make the discussion clearer. Films were kept in complete darkness and in a dry environment, in order to avoid any risk of hydrolysis or oxidation of the surface of the films.

Optical transmission spectra at normal incidence of the thin-film samples were obtained over the 400–2500 nm spectral range by a double-beam UV–vis–NIR spectrophotometer (Perkin-Elmer, model Lambda-19). The area of illumination over which a single transmission spectrum was obtained is 1 mm × 10 mm. Specular optical reflection spectra were also obtained at near-normal incidence (6 degrees of incidence), in the spectral range between 400 and 2200 nm, using the same spectrophotometer. The measuring-beam spot size was then set at 1 mm × 4 mm for practical reasons. Measurements of the total (specular plus diffuse) reflectance of all the samples were further taken in the same spectral range, using an integrating sphere installed in a double-beam UV–vis–NIR spectrophotometer (Perkin-Elmer, model Lambda-9). The surface roughness of the films was checked by means of a stylus-based profilometer (Sloan, model Dektak 3030).

3. Results

Fig. 1 shows the X-ray diffraction patterns of the thermally evaporated, PECVD-deposited and spin-coated amorphous $As_{40}S_{60}$ films. Note the presence of

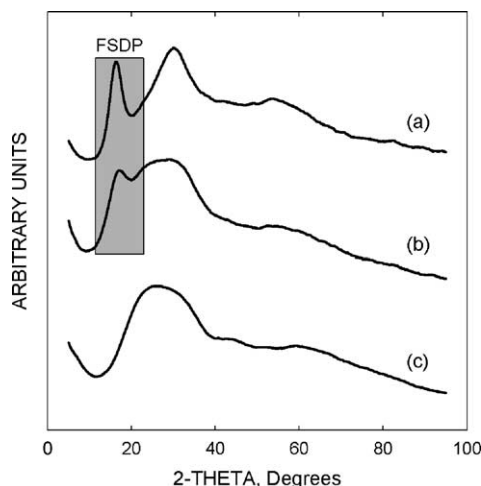


Fig. 1. X-ray diffraction patterns corresponding to a representative set of amorphous $\text{As}_{40}\text{S}_{60}$ films prepared by thermal evaporation (a), PECVD (b) and spin coating (c).

the so-called first sharp diffraction peak (FSDP) in those diffraction patterns of the thermally evaporated and PECVD-deposited samples at $2\theta = 16.02^\circ$ and 17.20° , respectively, which correspond to values of the modulus of the scattering vector, $Q \approx 1.1 \text{ \AA}^{-1}$, while the patterns of the spin-coated films do not show this feature. This characteristic feature in the X-ray diffraction results of amorphous chalcogenides has been traditionally associated with the existence of medium-range structural order in non-crystalline solids [1,9–13]. Among the different models suggested, stands out the one proposed by Elliott [11,12]. According to this model, the FSDP is due to the presence of an *ordered* pattern of interstitial voids in the amorphous matrix. In our particular case, this model would be interpreted with the presence of such a free volume surrounding AsS_3 pyramidal units.

The optical transmission spectra of a representative set of samples, prepared by the three different deposition techniques under consideration, are plotted in Fig. 2. The specular and total (specular + diffuse) reflection spectra of the sample prepared by spin coating are also shown in the inset of this figure. The shrinking observed in the amplitude of the interference fringes of the transmission spectra of both the thermally evaporated and PECVD-deposited samples, indicates the characteristic non-uniformity in thickness of films prepared by these two particular

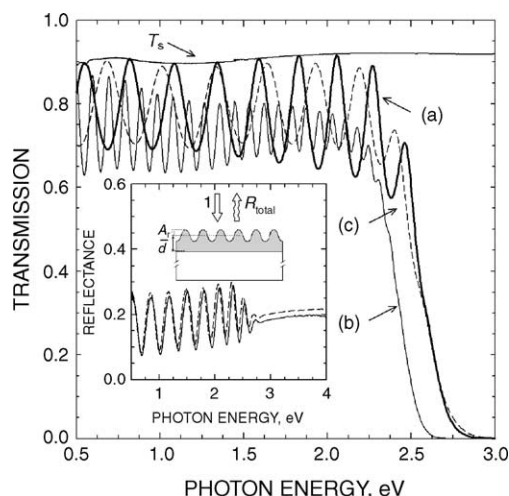


Fig. 2. Optical transmission spectra of thermally evaporated (a), PECVD-deposited (b) and spin-coated (c) amorphous $\text{As}_{40}\text{S}_{60}$ films. The transmission spectrum of the bare substrate, T_s , is also plotted in the graph. In the inset, it is shown the specular reflection spectrum (solid line) and the total reflection spectrum (dashed line) of a representative spin-coated film.

deposition techniques [2,14,15]. On the other hand, evidences of significant surface roughness have been found in the spin-coated films, from both the comparison of their specular and total reflection spectra, and the mechanical measurements carried out by the profilometer [16]. No indications of such a surface feature were observed in the films prepared by the other two techniques.

The optical and geometrical characterization of the samples was done by using the method most suitable to their thickness profile. Thus, two *envelope* methods developed by the authors, one based on the transmission spectra [17,18], and another based on the reflection spectra [16,19], both measured at normal (or near-normal) incidence, were used to calculate the refractive index, n , the absorption coefficient, α , and the average thickness, \bar{d} , of all the samples, as well as the wedging parameter, Δd , of the thermally evaporated and PECVD-deposited films, and the average surface roughness, A_r (see the inset in Fig. 2), of the spin-coated ones. In all cases, the accuracy in the determination of n and \bar{d} was better than 1%, and the values of the latter were cross-checked with those measured by use of the surface-profiling stylus instrument. Differences between the directly measured and the optically calculated values were less than 2%.

The set of values of the refractive index obtained from the application of the corresponding envelope method, at those wavelengths where the transmission (or reflection) spectra and their two envelopes are *tangential* [17,19], were analysed on the basis of the Wemple–DiDomenico (WDD) dispersion model [20,21], which is based on the single-oscillator approach:

$$n^2(\hbar\omega) = 1 + \frac{E_o E_d}{E_o^2 - (\hbar\omega)^2}, \quad (1)$$

where \hbar is Planck’s constant divided by 2π , $\hbar\omega$ the photon energy, E_o the single-oscillator energy and E_d is the dispersion energy or oscillator strength. Plotting $(n^2 - 1)^{-1}$ against $(\hbar\omega)^2$ allows one to determine the oscillator parameters by fitting a straight line to the experimental points, as shown in Fig. 3. Table 1 lists the values of the dispersion parameters for the amorphous $As_{40}S_{60}$ films under study, as well as the values for the static refractive index, $n(0)$, obtained by extrapolation of Eq. (1) towards $\hbar\omega = 0$. Fig. 3 clearly evidences the influence of the deposition technique in the refractive index of the thin-film samples: the PECVD-deposited samples show the largest values of n , while the spin-coated ones have the lowest. In all cases, the dispersion of the refractive index departs from the linear behaviour expected according to the above equation, when the photon energy goes out of the transparent region, as expected [20,21].

On the other hand, an important achievement of the WDD model is that it relates the dispersion energy, E_d , to other physical parameters of the material through the following empirical relationship [20,21]:

$$E_d \text{ (eV)} = \beta N_c Z_a N_e, \quad (2)$$

Table 1

Values of the average thickness, \bar{d} , wedging and surface-roughness indicating parameters, Δd and A_r , respectively, WDD dispersion parameters, E_o and E_d , the static refractive index, $n(0)$, Tauc gap, E_g^{opt} , Tauc slope, $B^{1/2}$, localised-state tail width, ΔE , and Urbach energy, E_c , for the amorphous $As_{40}S_{60}$ films prepared by the deposition techniques listed below

Deposition technique	\bar{d} (nm)	Thickness inhomogeneity (nm)	E_o (eV)	E_d (eV)	N_c	$n(0)$	E_g^{opt} (eV)	$B^{1/2}$ (cm ^{-1/2} eV ^{-1/2})	ΔE (meV)	E_c (meV)
Thermal evaporation	1098 ± 4	$\Delta d = 9 \pm 1$	5.11 ± 0.01	20.65 ± 0.04	3.0 ± 0.3	2.245 ± 0.001	2.43 ± 0.01	900 ± 2	73	84
PECVD	2646 ± 13	$\Delta d = 50 \pm 2$	4.90 ± 0.02	21.99 ± 0.07	3.2 ± 0.3	2.343 ± 0.001	2.37 ± 0.01	790 ± 2	88	113
Spin coating	814 ± 3	$A_r = 18 \pm 1$	5.13 ± 0.04	20.13 ± 0.16	2.9 ± 0.3	2.220 ± 0.001	2.37 ± 0.01	784 ± 1	99	118

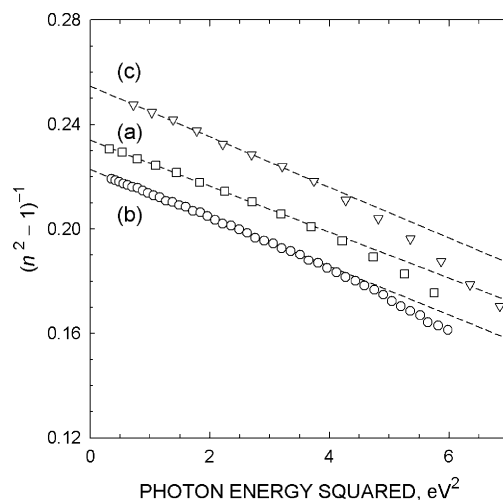


Fig. 3. Plot of the refractive-index factor $(n^2 - 1)^{-1}$ vs. $(\hbar\omega)^2$ for amorphous $As_{40}S_{60}$ films prepared by thermal evaporation (a), PECVD (b) and spin coating (c). Dashed lines are the corresponding least-square linear fits. As expected, the experimental dispersion of the refractive index departs from the linear behaviour given by Eq. (1) for photon energies outside the transparent region.

where N_c is the effective coordination number of the cation nearest-neighbour to the anion, Z_a the formal chemical valency of the anion, N_e the effective number of valence electrons per anion and β is a two-valued constant with either an ionic or a covalent value ($\beta_i = 0.26 \pm 0.03$ eV and $\beta_c = 0.37 \pm 0.04$ eV, respectively). Bearing in mind the mainly covalent character of the bonds forming the compounds being studied, as well as their chemical composition, namely, $As_{40}S_{60}$, the values $Z_a = 2$, $N_e = (40 \times 5 + 60 \times 6)/60 = 28/3$ and $\beta_c = 0.37 \pm 0.04$ eV, will be assumed to be constant in Eq. (2) when discussing the values obtained for the dispersion parameter E_d of the samples. Therefore, according to Eq. (2), any

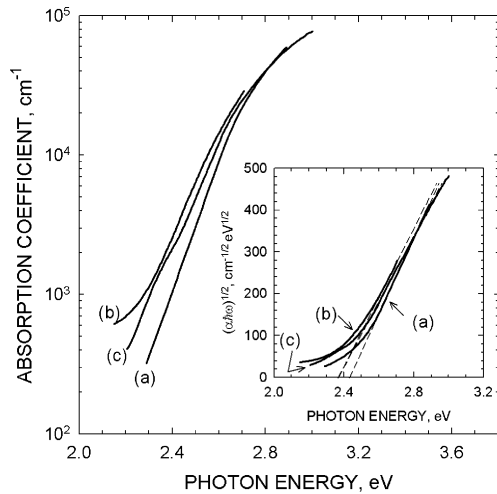


Fig. 4. Optical absorption spectra, $\alpha(\hbar\omega)$, of amorphous $\text{As}_{40}\text{S}_{60}$ films prepared by thermal evaporation (a), PECVD (b) and spin coating (c). Shown in the inset is the determination of the optical gaps in terms of Tauc's law as linear extrapolation of the strong absorption data (dashed lines).

difference in E_d , as a consequence of the deposition technique used, will be likely due to also differences in the As effective coordination number, N_c .

Values of the absorption coefficient, α , of the thin-film samples, in the strong absorption region ($\alpha \gtrsim 10^4 \text{ cm}^{-1}$), have been calculated in all cases from the upper envelope of the transmission spectra [15,17]. The calculated optical absorption spectra, $\alpha(\hbar\omega)$, for a representative set of amorphous $\text{As}_{40}\text{S}_{60}$ films, are displayed in Fig. 4, using a semi-logarithmic scale. Analysis of the strong absorption region has been carried out by the following well-known quadratic equation, which is often called the Tauc law [22,23]:

$$\alpha(\hbar\omega) = B \frac{(\hbar\omega - E_g^{\text{opt}})^2}{\hbar\omega}, \quad (3)$$

where B is a constant, which depends on the electronic transition probability and it is considered to be linked to the structural randomness of amorphous materials, and E_g^{opt} is the so-called Tauc gap. The values of $B^{1/2}$ and E_g^{opt} for the thermally evaporated, spin-coated and PECVD-deposited amorphous $\text{As}_{40}\text{S}_{60}$ films have been derived by plotting $(\alpha\hbar\omega)^{1/2}$ versus $\hbar\omega$ (see the inset in Fig. 4), and they all are listed in Table 1.

4. Discussion

It is well known [1] that the structure of As_2Ch_3 binary amorphous chalcogenides (Ch being a chalcogen atom) consists of locally two-dimensional structural layers, formed by AsCh_3 pyramidal units linked through a common two-fold coordinated chalcogen atom, and interacting with each other by weak intermolecular bonds. According to Wemple [21], interactions between structural layers through As atoms acting as bonding points, forming $\text{As}\cdots\text{Ch}$ intermolecular bonds, would contribute to increase the As effective coordination number, and thus $N_c > 3$ is expected. Particularly, for $\text{As}_{40}\text{S}_{60}$ bulk glass, Wemple suggests a value of $N_c \approx 3.2$.

On the other hand, it is also well known that deposition techniques such as vacuum thermal evaporation and PECVD lead to the formation of molecular clusters during the deposition process (e.g., quasi-spherical As_4S_4 , and S_n and As_4 molecular fragments), which eventually remain embedded in the film amorphous matrix. These molecular clusters would make difficult the cohesion between the structural layers, and consequently, would contribute to increase the free volume around the structural bricks formed by the AsS_3 pyramidal units, and in turn, to decrease the As effective coordination number, N_c . This could explain the difference between the value of N_c found for all our amorphous $\text{As}_{40}\text{S}_{60}$ films (see Table 1), and the value proposed by Wemple [21] for the $\text{As}_{40}\text{S}_{60}$ bulk glass, $N_c \approx 3.2$.

Therefore, according to Wemple's ideas, the differences observed in E_d (and consequently, in N_c), in samples prepared by different deposition techniques, point towards a stronger interaction between structural layers forming the amorphous network of PECVD-deposited samples, while this interaction being weaker in the case of spin-coated films. It is important to note that even though the differences inferred for N_c are almost within the error bars (see Table 1), we believe that the differences in E_d , on which the above conclusion is based, are undoubtedly significant. This conclusion is also supported by the X-ray diffraction experiments, which further suggest the greater presence of molecular clusters in the thermally evaporated amorphous films, in comparison with the PECVD-deposited ones, based on the higher intensity of the FSDP in the X-ray diffraction patterns of the former.

On the other hand, the above-mentioned molecular fragments are not expected to be present in the spin-coated films, as this particular technique does not involve any new chemical reaction between As and S species during the preparation of the solution in *n*-propylamine. Hajto et al. [24,25] have shown by IR spectroscopic measurements that solvent molecules are linked to S atoms through the $-\text{NH}_2$ amine radical, in such a fashion that even thermally stabilized, the spin-coated films still contain *n*-propylamine molecules in the chalcogenide matrix breaking the *continuous random network* model expected for these films. Thus, the presence of the solvent molecules would contribute to increase the structural randomness in the spin-coated films, further *filling in* the voids around the AsS_3 pyramidal units. This could explain the total absence of the FSDP in the X-ray diffraction patterns corresponding to the spin-coated films, as well as the low value of N_c (2.9) found for these samples.

Values of the refractive index of the amorphous $\text{As}_{40}\text{S}_{60}$ films, prepared by the different deposition techniques considered in the present work, are consistent with all the comments on the structure of the films stated above. In fact, the highest compactness of the PECVD-deposited films, as inferred from their X-ray diffraction patterns and further supported by the value found for N_c , leads to large values of the refractive index, as expected from the Lorentz–Lorenz relationship [26]. On the other hand, the presence of low refractive-index ($n(\lambda = 589.3 \text{ nm}) = 1.388 \pm 0.005$ [27]) solvent remains in the spin-coated films, leads to a decrease in the overall value of n for these films in comparison with the thermally evaporated and PECVD-deposited samples.

Following the discussion on the role played by the deposition technique in the optical properties of amorphous $\text{As}_{40}\text{S}_{60}$ films, the optical absorption spectra of these samples, shown in Fig. 4, will be analysed. From this figure can be concluded that the PECVD-deposited $\text{As}_{40}\text{S}_{60}$ semiconducting films are more absorbing than their spin-coated and thermally evaporated counterparts. The largest value of E_g^{opt} for the thermally evaporated films could plausibly be explained on the basis of the presence of the above-mentioned homopolar bond containing molecular clusters. Taking into account that the bonding energies of S–S and As–As bonds are greater than that corresponding to the As–S heteropolar bond, the

presence of such clusters in the amorphous matrix will contribute to increase the value of E_g^{opt} . The low value of E_g^{opt} for the PECVD-deposited films can also be explained under this assumption, as they have a lower content of homopolar bond containing molecular clusters, as deduced from their X-ray diffraction results. Spin-coated films, on the contrary, compensate the absence of molecular clusters by the presence of *n*-propylamine molecules, in such a fashion that the carbon bonds increase slightly their optical absorption.

Finally, as already mentioned, the parameter B in Eq. (4) is assumed to be an indicator of the degree of structural randomness of amorphous semiconductors [28–30], and it is related with the localised-state tail width, ΔE , through the following relationship suggested by Mott and Davis [28]:

$$B = \frac{4\pi\sigma_{\min}}{n(0)c\Delta E} \quad (4)$$

where σ_{\min} is the minimum electrical conductivity, $n(0)$ the already-introduced static refractive index and c is the light speed in vacuum. Bearing in mind the idea that ΔE would be null for crystalline semiconductors, it is straightforward inferred from the above equation that the smaller the B value, the higher the structural disorder. Assuming $\sigma_{\min} = 350 \Omega^{-1}$ as a typical value for amorphous $\text{As}_{40}\text{S}_{60}$ alloys [30], it is possible to estimate the influence of the deposition technique in the localised-state tail widths of the amorphous semiconducting films under study. Values of $B^{1/2}$, derived from the Tauc's plots shown in the inset of Fig. 4, and ΔE , calculated from Eq. (4), are all listed in Table 1. From these results, it is concluded that the thermally evaporated amorphous films show the highest degree of structural order, probably because of the presence of As_4S_4 molecular clusters, while the spin-coated ones are the most disordered structurally.

On the other hand, the optical absorption edges ($\alpha \gtrsim 10^4 \text{ cm}^{-1}$) follow, as expected, the Urbach rule [31]:

$$\alpha(\hbar\omega) = \alpha_0 \exp\left(\frac{\hbar\omega}{E_c}\right) \quad (5)$$

where α_0 is a pre-exponential factor and E_c is the so-called Urbach energy. The latter parameter has also been related with the structural disorder of amorphous semiconductors [29,32–34], in such a fashion that

$E_c \rightarrow 0$ for crystalline semiconductors. It is worth noting that UV–vis–NIR transmission spectroscopy is not the most appropriate technique to get accurate information of such a low absorption region, photo-thermal deflection spectroscopy being the most suitable one instead. Nevertheless, the technique used in the present work provides significant values in the range 10^3 – 10^4 cm^{-1} . Therefore, it has been proceeded to analyse such a range of data in order to estimate, at least, the E_c values of our samples, and to check their coherence with the $B^{1/2}$ values obtained. In fact, it has been found that E_c values support the conclusions derived from the $B^{1/2}$ values (see Table 1).

Lastly, it is important to quote the work carried out by Zanatta and Chambouleyron [29], who tried to establish a relationship between these two indicators of the degree of structural disorder of amorphous solids. Thus, they found a linear relationship between them when studying the optical properties of both nitrogen-doped amorphous Ge:H and Si:H films: The analytical expressions being $E_c = -0.36B^{1/2} + 347$ and $E_c = -0.22 B^{1/2} + 240$, respectively. The least-square fit of the results reported in the present work gave $E_c = -0.26 B^{1/2} + 318$ (correlation coefficient $r = 0.93$), which seems to be in good agreement with the above-introduced ones. Nevertheless, it would be necessary to compile a greater set of data from films with different compositions, and prepared under different conditions, before reaching a conclusion on the dependence between E_c and $B^{1/2}$ in the case of amorphous chalcogenide semiconductors.

5. Concluding remarks

Amorphous $\text{As}_{40}\text{S}_{60}$ films have been successfully prepared by vacuum thermal evaporation, PECVD and spin coating. The optical characterization of the thin-film samples was carried out by using the envelope method most suitable to the film thickness profiles. Thermally evaporated and PECVD-deposited films showed wedge-shaped profiles, while a significant surface roughness was observed in the spin-coated ones. The average-thickness and refractive-index values were calculated with accuracies better than 1% in all cases.

Structural features of these films have been derived both from X-ray diffraction experiments and from the

analysis of the dispersion of the refractive index. It has been found a notable influence of the deposition technique in the structural and optical properties of the amorphous $\text{As}_{40}\text{S}_{60}$ films. Thus, PECVD leads to highly compact films with low concentration of homopolar bond containing molecular clusters, which reflects in their high refractive-index values. Thermally evaporated samples contain a higher concentration of molecular clusters, which explains the higher intensity found for the FSDP. Finally, spin-coating deposition does not produce such clusters, but the solvent remains have a great influence on the structural and optical properties of these films, increasing, on one hand, the degree of structural randomness, and decreasing, on the other hand, the refractive index.

Finally, the analysis of the optical absorption spectra of these amorphous semiconducting films has allowed obtaining the values of their optical band gaps, as well as, getting information about the degree of structural disorder of these films from both the Tauc slope, $B^{1/2}$, and Urbach energy, E_c .

Acknowledgements

This work has been partly supported by the MCYT (Spain) and FEDER (CEE) under MAT2001-3333 research project, and a Marie Curie European Reintegration Grant of the Sixth Framework Programme under contract number MERG-CT-2004-507791.

References

- [1] S.R. Elliott, *Physics of Amorphous Materials*, second ed. Longman, London, 1990.
- [2] R. Glang, in: L.I. Maissel, R. Glang (Eds.), *Handbook of Thin Film Technology*, McGraw-Hill, New York, 1983.
- [3] G. Myburg, R. Swanepoel, *J. Non-Cryst. Solids* 89 (1987) 13.
- [4] M. Popescu, *Non-Crystalline Chalcogenides*, Kluwer Academic Publishers, Dordrecht, 2000.
- [5] A. Kolobov, K. Tanaka, Photo-induced phenomena in amorphous chalcogenides: from phenomenology to nanoscale, in: H.S. Nalwa (Ed.), *Handbook of Advanced Electronic and Photonic Materials and Devices*, vol. 5, Academic Press, San Diego, 2001.
- [6] A.V. Kolobov, in: A.V. Kolobov (Ed.), *Photo-Induced Metastability Amorphous Semiconductors*, Wiley-VCH, Weinheim, 2003.

- [7] During the deposition process, the substrates were conveniently rotated by means of a planetary rotation system, which makes possible to reduce, to some extent, the lack of uniformity in the thickness of the as-deposited glass films. The deposition rate was kept in the range $1\text{--}8\text{ nm s}^{-1}$, measured continuously using the quartz microbalance technique
- [8] Before the deposition, the solution was filtered with a $0.5\text{ }\mu\text{m}$ filter in order to remove, to some extent, any undissolved material. The spin speed was maintained at 3000 rpm, during 20 s. The films were annealed under nitrogen, at a temperature of $90\text{ }^\circ\text{C}$ (well below the glass transition temperature, $T_g = 180\text{ }^\circ\text{C}$), for 30 min to remove any solvent that could be present
- [9] S.R. Elliott, in: J. Zarzycki (Ed.), *Materials Science and Technology*, vol. 9, VCH, New York, 1991.
- [10] A.A. Vaipolin, E.A. Porai-Koshits, *Sov. Phys.-Solid State* 5 (1963) 497.
- [11] S.R. Elliott, *Nature* 354 (1991) 445.
- [12] S.R. Elliott, *Phys. Rev. Lett.* 67 (1991) 711.
- [13] Ke. Tanaka, *Jpn. J. Appl. Phys.* 37 (1998) 1747.
- [14] E. Márquez, P. Nagels, J.M. González-Leal, A.M. Bernal-Oliva, E. Sneeckx, R. Callaerts, *Vacuum* 52 (1998) 55.
- [15] R. Swanepoel, *J. Phys. E: Sci. Instrum.* 17 (1984) 896.
- [16] J.M. González-Leal, R. Prieto-Alcón, M. Stuchlik, M. Vlcek, S.R. Elliott, E. Márquez, *Opt. Mater.* 27 (2004) 147.
- [17] J.M. González-Leal, R. Prieto-Alcón, J.A. Ángel, D.A. Minkov, E. Márquez, *Appl. Opt.* 41 (2002) 7300.
- [18] J.M. González-Leal, R. Prieto-Alcón, M. Vlcek, E. Márquez, *J. Non-Cryst. Solids* 345–346 (2004) 88.
- [19] J.J. Ruiz-Pérez, J.M. González-Leal, D.A. Minkov, E. Márquez, *J. Phys. D: Appl. Phys.* 34 (2001) 2489.
- [20] S.H. Wemple, M. DiDomenico, *Phys. Rev. B* 3 (1971) 1338.
- [21] S.H. Wemple, *Phys. Rev. B* 7 (1973) 3767.
- [22] J. Tauc, A. Menth, *J. Non-Cryst. Solids* 8–10 (1972) 569.
- [23] J. Tauc, in: J. Tauc (Ed.), *Amorphous and Liquid Semiconductors*, Plenum Press, New York, 1974.
- [24] E. Hajto, P.J.S. Ewen, R. Belford, J. Hajto, A.E. Owen, *J. Non-Cryst. Solids* 97–98 (1987) 1191.
- [25] E. Hajto, Ph.D. Thesis, University of Edinburgh, 1991.
- [26] S.R. Elliott, *The Physics and Chemistry of Solids*, Wiley, Chichester, 2000.
- [27] R.R. Dreisbach, *Physical Properties of Chemical Compounds*, vol. III, American Chemical Society, Washington, 1961.
- [28] N.F. Mott, E.A. Davis, *Electronic Processes in Non-Crystalline Materials*, second ed. Clarendon Press, Oxford, 1979.
- [29] A.R. Zanatta, I. Chambouleyron, *Phys. Rev. B* 53 (1996) 3833.
- [30] L. Tichy, H. Ticha, P. Nagels, R. Callaerts, *Mater. Lett.* 36 (1998) 294.
- [31] F. Urbach, *Phys. Rev. B* 92 (1953) 1324.
- [32] S. Abe, Y. Toyozawa, *J. Phys. Soc. Jpn.* 50 (1981) 2185.
- [33] C.M. Soukoulis, M.H. Cohen, E.N. Economou, J.L. Souquet, *Phys. Rev. Lett.* 53 (1984) 616.
- [34] G.D. Cody, in: J.I. Pankove (Ed.), *Semiconductors and Semimetals*, vol. 21B, Academic Press, New York, 1984.